Glycochenodeoxycholate-induced Lethal Hepatocellular Injury in Rat Hepatocytes

Role of ATP Depletion and Cytosolic Free Calcium

James R. Spivey, Steven F. Bronk, and Gregory J. Gores
Center for Basic Research in Digestive Diseases, Department of Internal Medicine, Mayo Medical School, Clinic and Foundation, Rochester, Minnesota 55905

Abstract

Chenodeoxycholate is toxic to hepatocytes, and accumulation of chenodeoxycholate in the liver during cholestasis may potentiate hepatocellular injury. However, the mechanism of hepatocellular injury by chenodeoxycholate remains obscure. Our aim was to determine the mechanism of cytotoxicity by chenodeoxycholate in rat hepatocytes. At a concentration of 250 μM, glycochenodeoxycholate was more toxic than either chenodeoxycholate or taurochenodeoxycholate. Cellular ATP was 86% depleted within 30 min after addition of glycochenodeoxycholate. Fructose, a glycolytic substrate, maintained ATP concentrations at 50% of the initial value and protected against glycochenodeoxycholate cytotoxicity. ATP depletion in the absence of a glycolytic substrate suggested impairment of mitochondrial function. Indeed, glycochenodeoxycholate inhibited state 3 respiration in digitonin-permeabilized cells in a dose-dependent manner. After ATP depletion, a sustained rise in cytosolic free calcium (Ca_i^{2+}) was observed. Removal of extracellular Ca^{2+} abolished the rise in Ca_i^{2+}, decreased cellular proteolysis, and protected against cell killing by glycochenodeoxycholate. The results suggest that glycochenodeoxycholate cytotoxicity results from ATP depletion followed by a subsequent rise in Ca_i^{2+}. The rise in Ca_i^{2+} leads to an increase in calcium-dependent degradative proteolysis and, ultimately, cell death. We conclude that glycochenodeoxycholate causes a bioenergetic form of lethal cell injury dependent on ATP depletion analogous to the lethal cell injury of anoxia. (*J. Clin. Invest.* 1993. 92:17–24.) Key words: ATP • bile salts • cytosolic free calcium • fructose • proteolysis

Introduction

Bile salts are transported into the hepatocyte by a specific transport protein on the sinusoidal plasma membrane, vectorially transported across the cell, and excreted by the hepatocyte canalicular membrane into bile. Cholestasis, the impairment of bile flow, inhibits excretion of bile salts into bile, leading to an accumulation of bile salts within the hepatocyte. Intracellular accumulation of bile salts by the hepatocyte during cholestasis is thought to play a pivotal role in cholestatic liver injury. Indeed, bile salts have been shown to be cytotoxic for hepatocytes, intestinal epithelial cells, and mast cells (1–5). Recent data demonstrating that ursodeoxycholate (the 7-beta epimer of the primary bile salt chenodeoxycholate [CDC][1]) ameliorates human cholestatic liver disease have stimulated renewed interest in the cellular mechanisms of lethal bile salt injury (6–11). Because bile salts are detergents and form micelles, bile acid cytotoxicity has been attributed to their detergent properties (1, 7, 8). However, changes in cytosolic free calcium (Ca_i^{2+}) and ATP have also been proposed as nondetergent mechanisms for bile salt–associated cytotoxicity. Indeed, toxic bile salts cause hemolysis of ATP-depleted red blood cells by a calcium-dependent mechanism (12). Moreover, monohydroxylated bile salts lead to an increase in Ca_i^{2+} by releasing calcium from intracellular stores at concentrations of only 100 μM (13), and dihydroxylated bile salts have been demonstrated to increase the permeability of synthetic membranes and biomembranes to calcium and cause an increase in Ca_i^{2+} in hepatocytes (14–17). A sustained increase in Ca_i^{2+} has been proposed as a common mechanism of cell death by activating calcium-dependent degradative hydrolases, including proteases, phospholipases, and endonucleases (18, 19). Thus, bile salt cytotoxicity may be mediated by changes in cellular ATP and calcium concentrations.

A likely candidate for bile salt–mediated hepatocellular injury during cholestasis is CDC. CDC, a primary bile salt, is known to be directly cytotoxic for hepatocytes (20). Hepatic concentrations of CDC increase 20-fold during cholestasis (21). CDC is > 95% conjugated to glycine or taurine in bile during cholestasis with a glycine/taurine ratio of 3:2, and glycine conjugates of toxic bile salts are generally more toxic than taurine conjugates (1, 22, 23). In addition, hepatic tissue concentrations of CDC during cholestasis are greater than those of other toxic bile salts such as lithocholate and deoxycholate (21). This information indicates that the mechanisms of CDC-mediated cytotoxicity are of potential clinical importance. However, information is lacking regarding the cellular mechanisms mediating lethal hepatocellular injury by CDC. Thus, our aim was to determine the mechanisms of glycochenodeoxycholate(GCDC)-mediated lethal hepatocellular injury using rat hepatocytes.

Preliminary portions of this work were presented at the 93rd meeting of the American Gastroenterological Association and published in abstract form (1992. *Gastroenterology.* 102:A892).

Address correspondence to Dr. Gregory J. Gores, Associate Professor of Medicine, Center for Basic Research in Digestive Diseases, Mayo Medical School, Clinic, and Foundation, Rochester, MN 55905.

Received for publication 16 July 1992 and in revised form 20 January 1993.

1. *Abbreviations used in this paper:* Ca_i^{2+}, cytosolic free calcium; CDC, chenodeoxycholate; GCDC, glycochenodeoxycholate; KRH, Krebs-Ringers-Hepes; TCDC, taurochenodeoxycholate; TMRE, tetramethylrhodamine ethyl ester; TUDC, tauroursodeoxycholate.

Methods

Cell isolation and culture. The use and care of the animals for these studies were reviewed and approved by the Institutional Animal Care and Use Committee at the Mayo Clinic. Hepatocyte suspensions were isolated from adult male Sprague-Dawley rats (250–350 g) as previously described in detail (24, 25). For culturing, hepatocytes were resuspended in culture medium at 250,000 cells/ml. 1-ml aliquots were cultured in 35 × 10-mm Petri dishes (Becton Dickinson Labware; Becton Dickinson, Lincoln Park, NJ) on 22-mm square glass coverslips coated with type I collagen from rat tail tendon (24). The culture medium was Waymouths 752/1 containing 10% FCS and 100 nM insulin. Hepatocytes were used after 2 h of culture in 5% CO_2/air at 37°C. We chose to study hepatocytes after 2 h in culture for the following reasons. First, hepatocytes are known to dedifferentiate rapidly in culture. Indeed, hepatocytes cultured overnight transport bile acids less efficiently than freshly isolated hepatocytes (26). Second, in establishing our experimental model, we wanted to duplicate the published results demonstrating transient increases in Ca_i^{2+} from an inositol triphosphate–sensitive intracellular pool by taurolithocholate (13). We were not able to repeat these published results in cells cultured overnight, presumably due to inefficient bile salt transport by these cells, but were able to obtain similar results in cells cultured for 2 h. Finally, we wanted to use freshly cultured cells because the results with these cells would most closely parallel those experiments using freshly isolated hepatocyte suspensions.

Solutions. The basic incubation medium was Krebs-Ringers-Hepes (KRH) buffer, pH 7.4 (24). Mitochondrial oxygen consumption was measured in digitonin-permeabilized hepatocytes in a buffer containing 125 mM sucrose, 50 mM KCl, 1 mM EGTA, 1 mM MgCl, 2 mM KH_2PO_4, 5 mM Hepes, and 10 μM digitonin. Fura-2-AM, tetramethylrhodamine ethyl ester (TMRE), and compound 1799 were stored in DMSO as 1-mM solutions at −20°C.

Determination of cell viability. Cell viability was determined from the total fluorescence of propidium iodide (27). Fluorescence was monitored using a filter fluorometer (model 450; Sequoia-Turner, Mountain View, CA) with 520-nm (8-nm band pass) excitation and 605-nm (long pass) emission filters.

Determination of unbound bile salt concentrations. Unbound bile salt concentrations were estimated by ultrafiltration (28). A 1-ml aliquot of the cell suspension mixture was added to a MPS-1 unit (Amicon, Beverly, MA) and passed through a YMT ultrafiltration membrane by centrifugation at 900 *g* for 25 min (Mistral 3000i centrifuge; Curtin Matheson Scientific, Houston, TX). The resulting ultrafiltrate was diluted 1:10 with KRH buffer. GCDC concentrations were measured in the ultrafiltrate fluorometrically as described by Mashige et al. (29). Fluorescence was quantitated in a luminescence spectrometer/fluorometer (model LS-50; Perkin-Elmer Corp., Norwalk, CT). It should be noted that actual unbound bile acid concentrations may be somewhat lower than concentrations in an ultrafiltrate because of Gibbs-Donnan effects.

ATP measurements. ATP was quantitated in hepatocyte suspensions by the luciferin/luciferase assay as we have previously described in detail (24). Bioluminescence was quantitated in a luminescence spectrometer/fluorometer (model LS-50; Perkin-Elmer Corp.).

Multiparameter digitized video microscopy. Experiments measuring mitochondrial membrane potential and Ca_i^{2+} were performed using a multiparameter digitized video microscopy system employing the Image-1/FL quantitative fluorescence software package from Universal Imaging Corp. (West Chester, PA) (24). The microscope is an inverted phase/fluorescence microscope (Axiovert 35M; Carl Zeiss, Inc., Thornwood, NY) equipped with a thermostat-controlled heated stage. Excitation light is provided by a 100-W mercury vapor lamp for measuring mitochondrial membrane potential and a 75-W Xe lamp for measuring Ca_i^{2+} and passed through an interference and neutral density filter wheel assembly (Eastern Microscope, Research Triangle Park, NC) to select wavelength and intensity under computer control. A shutter, also under computer control, automatically blocked the excitation light source between fluorescent measurements. A silicon-intensified target video camera (model 2400-08; Hamamatsu, Hamamatsu City, Japan) collects fluorescent images that are fed to a computer (Compaq 386-20E; Compaq Computer Corp., Houston, TX) and digitized with video acquisition and display boards (Matrox International Corp., Dorval, Quebec, Canada) for frame averaging, background subtraction, ratioing, and storage on a hard disk. Images were transferred to an optical disk drive for long-term storage (model SMO-S501; Sony Corp., Komoro, Japan).

Dye loading. Fura-2 was loaded into cultured hepatocytes in culture medium with 5 μM fura-2-acetoxymethylester for 30 min at 37°C. TMRE was loaded by incubating cultured hepatocytes in culture medium with 100 nM TMRE for 10 min at 37°C. In all instances, cells were washed three times with KRH buffer to remove extracellular dye.

Measurement of Ca_i^{2+}. Ca_i^{2+} was quantitated by ratio imaging of fura-2 fluorescence excited at 340 and 380 nm (24). Fluorescence was imaged through a 395-nm dichroic reflector and a 470–550 emission filter. The mean values of pixel ratios for individual cells are converted to Ca^{2+} using the calculation described by Grynkiewicz et al. using a K_d of 224 nM for the fura-2-Ca^{2+} complex (30). The values for R_{min}, R_{max}, and the constant Sf_2/Sb_2 are calculated from measurements with fura-2 free acid solutions in capillary tubes (internal diameter of 20 μm [Vitro Dynamics, Inc., Rockaway, NJ] placed on the microscope stage.

Measurement of mitochondrial membrane potential. The mitochondrial membrane potential was monitored using the membrane potential–sensitive dye TMRE and digitized video microscopy (24). TMRE is a fluorescent lipophilic cation that electrophoretically redistributes across the mitochondrial membrane according to the mitochondrial membrane potential. The exclusivity of TMRE localization to mitochondria has been demonstrated using confocal microscopy by Loew and co-workers (31). The mitochondrial membrane potential was monitored from TMRE fluorescence using a 546-nm excitation filter, a 580-nm dichroic reflector, and a 590-nm long-pass filter. Cells loaded with TMRE were incubated on the microscope stage with KRH containing 50 nM TMRE at 37°C. Cellular fluorescence was quantitated by multiplying the average fluorescence intensity in the cell by the number of pixels above background using a threshold of zero.

Measurement of mitochondrial respiration in digitonin-permeabilized cells. Hepatocytes were permeabilized with digitonin and mitochondrial respiration quantitated as described by Moreadith and Fiskum (32). Briefly, hepatocytes were added to respiration buffer containing 10 μM digitonin at a concentration of 0.5×10^6/ml. At this concentration of digitonin and cells the plasma membrane is rapidly permeabilized by digitonin, but the mitochondrial membrane is left intact (32). Oxygen consumption was measured using an air-tight chamber (model 5301; Yellow Springs Instrument Co., Yellow Springs, OH) with a biological oxygen monitor (model 5300; Yellow Springs Instrument Co.) equipped with an oxygen sensor (model 5331; Yellow Springs Instrument Co.). A strip chart recorder was used to monitor the rate of oxygen consumption over time. Temperature was maintained at 37°C using a circulating water bath. State 3 respiration was measured in the presence of 5 μM rotenone, 5 mM succinate, and 1 mM ADP (32). State 4 respiration was measured under identical conditions as state 3 except oligomycin, 1 μg/ml, was added to the buffer (32). The acceptor control ratio was defined as the rate of state 3 respiration divided by the rate of state 4 respiration.

Measurements of proteolysis. Hydrolysis of proteins results in the exposure of a primary amino group for every peptide bond broken (except bonds to proline). Measurement of the free primary amines provides a sensitive method to measure proteolysis. We used fluorescamine, a reagent that reacts with primary amines to form a fluorescent product, to quantitate proteolysis in cell suspensions using a slight modification of the technique of Pacifici and Davies, as we previously described (24, 33).

Statistical analysis. All data represent a minimum of three separate experiments performed in triplicate and are expressed as mean±standard error of the mean unless otherwise indicated. Differences between groups were analyzed using an analysis of variance for repeated mea-

sures and a post hoc Bonferroni test to correct for multiple comparisons. All statistical analyses were performed with the software package Instat (Graphpad, San Diego, CA) using an Epson personal computer (model Equity III+; Seiko Epson Corp., Torrance, CA).

Materials. Fluorescamine, ATP assay mix, propidium iodide, TCA, rotenone, ADP, succinate, 3α-hydroxysteroid dehydrogenase, diaphorase, resazurin, β nicotinamide adenine dinucleotide, polyethylene glycol (PEG; 1,000 mol wt), D-xylose, oligomycin, DNAse, pronase, and Fraction V of BSA were obtained from Sigma Chemical Co. (St. Louis, MO); Hepes buffer was obtained from United States Biochemical Corp. (Cleveland, OH); collagenase type D was obtained from Boehringer Mannheim Biochemicals (Indianapolis, IN); digitonin, tauroursodeoxycholate (TUDC), chenodeoxycholate, GCDC, and taurochenodeoxycholate (TCDC) were obtained from Calbiochem Corp. (La Jolla, CA). All bile salts were > 96% pure by thin layer chromatography performed by the manufacturer and were used without further purification. TMRE, fura-2, and fura-2-acetoxymethylester (fura-2-AM) were obtained from Molecular Probes, Inc. (Eugene, OR). Compound 1799 was a generous gift of P. G. Heytler (E.I. DuPont, Bloomington, DE). All other reagents were of analytical grade from the usual commercial sources.

Results

GCDC is the most toxic form of CDC. Because GCDC is the most prevalent form of CDC in bile during cholestasis, we first determined the dose–response curve for cell killing by GCDC. Loss of cell viability in hepatocyte suspensions during exposure to GCDC was dose dependent with near maximal toxicity observed at a concentration of 250 μM over the dose range studied, 0–500 μM GCDC (Fig. 1). Using a concentration of 250 μM for all three bile salts, GCDC was the most toxic of the CDC species, followed by CDC with minimal toxicity observed for TCDC (Fig. 2). Indeed, after 2 h of incubation, cell viability was only 23±1% with GCDC compared with a viability rate of 66±1% for CDC and 71±1% for TCDC ($P < 0.01$). Rat hepatocytes convert the hydrophobic bile salt CDC to the more hydrophilic bile salt muricholic acid. However, concentrations of muricholate of 250 μM were not toxic in our experiments.

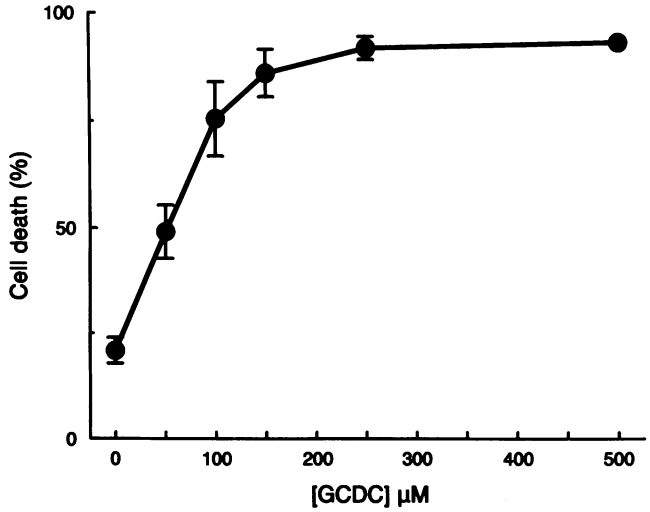

Figure 1. Concentration dependence of GCDC cytotoxicity. Hepatocyte suspensions (10^5/ml) were incubated in 3 ml of KRH buffer containing 1 μM propidium iodide and 0.2% BSA at 37°C. Cells were treated with increasing concentrations of GCDC and cell viability was assessed by propidium iodide fluorometry after 4 h.

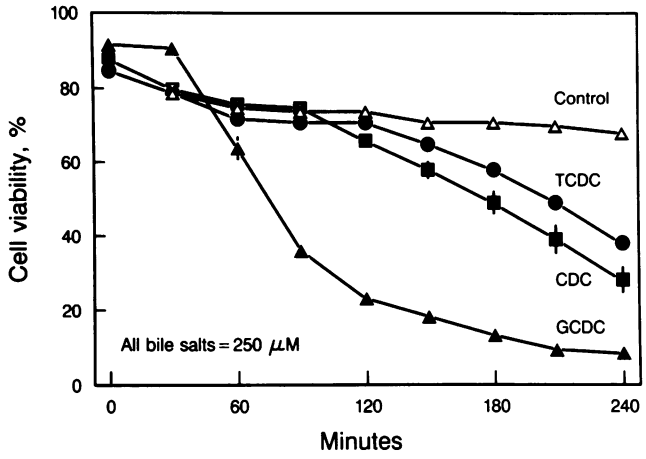

Figure 2. GCDC is more cytotoxic than TCDC or CDC. Hepatocyte suspensions (10^5/ml) were incubated in 3 ml of KRH buffer containing 1 μM propidium iodide and 0.2% BSA at 37°C. Cell viability was assessed by propidium iodide fluorometry after the addition of 250 μM GCDC (*closed triangles*), CDC (*closed squares*), TCDC (*closed circles*), or no addition (*open triangles*).

Thus, the toxicity of CDC could not be explained by intracellular conversion to muricholate. Because cytotoxicity was observed with 250 μM GCDC, we used this concentration and conjugate of CDC for the remainder of our experiments. At this concentration of GCDC, the free bile salt concentration varied little over the 4-h time period and was 78±9, 89±12, 96±17, 91±8, and 82±15 μM at 0, 1, 2, 3, and 4 h after the addition of GCDC to the cell suspensions (data not shown).

Fructose protects against ATP depletion and cell killing by GCDC. In hepatocyte suspensions exposed to GCDC, a rapid and substantial net hydrolysis of ATP was observed (Fig. 3). Cellular ATP concentrations were 86±5% depleted after 30 min. However, 250 μM TUDC had no effect on cellular ATP concentrations (Fig. 3). High concentrations of fructose have been shown to prevent total ATP depletion during cell injury by enhancing glycolytic generation of ATP (34). Therefore, we determined the effect of fructose on hepatocellular ATP concentrations during cytotoxicity by GCDC (Fig. 3). In the presence of 20 mM fructose, ATP concentrations initially fell to 30±2% of the initial value after 45 min and then increased and remained at values of 49±6% of the initial value thereafter (Fig. 3). The fructose-associated biphasic changes in cellular ATP concentration during cell injury are incompletely understood, but have been previously described (35). In addition to protecting against ATP depletion, fructose also protected against GCDC cytotoxicity (cell viability of 23±1% without fructose vs. 74±2% with fructose after 2 h of exposure to GCDC, $P < 0.01$, Fig. 4). In contrast, isosmotic replacement of fructose with 20 mM PEG (Fig. 4) or 20 mM D-xylose (data not shown) did not protect against GCDC cytotoxicity. Thus, fructose protects against ATP depletion and cell killing by GCDC, suggesting that ATP depletion plays a critical role in mediating GCDC cytotoxicity.

GCDC impairs mitochondrial function. Loss of cellular ATP depletion during GCDC cytotoxicity suggested loss of mitochondrial or glycolytic ATP generation. However, production of ATP by fructose, a glycolytic substrate, indicates that glycolytic pathways are intact. Therefore, we directly assessed the effect of GCDC on mitochondrial function using two ap-

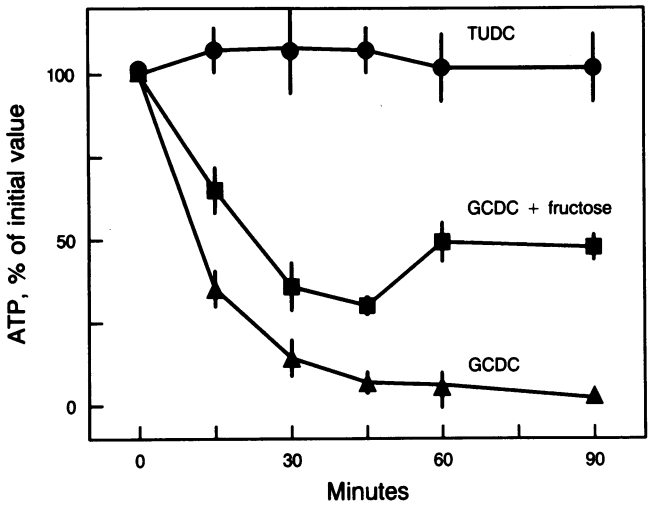

Figure 3. Fructose ameliorates ATP depletion by GCDC. Hepatocyte suspensions (106/ml) were incubated in 3 ml of KRH buffer containing 0.2% BSA at 37°C. Cells were incubated in the presence of 250 μM GCDC (*closed triangles*), 250 μM GCDC plus 20 mM fructose (*closed squares*), and 250 μM TUDC (*closed circles*). ATP concentrations were quantitated using a luciferin/luciferase bioluminescence assay. Basal concentrations of ATP were 19.8±1.2 nmol/106 cells.

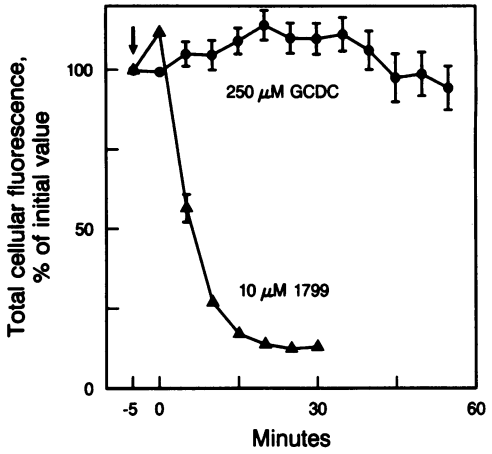

Figure 5. Lack of effect of GCDC on the mitochondrial membrane potential. The mitochondrial membrane potential was monitored in isolated, cultured hepatocytes from TMRE fluorescence using multiparameter digitized video microscopy. Total cellular fluorescence was monitored before and after treatment with 250 μM GCDC (*closed circles*) and 10 μM compound 1799 (*closed triangles*), a nonfluorescent mitochondrial uncoupler.

proaches: (*a*) we determined the effect of GCDC on the mitochondrial membrane potential in situ using cultured hepatocytes; and (*b*) we determined the effect of GCDC on mitochondrial respiration using permeabilized cell suspensions. After the addition of 250 μM GCDC, there was no significant change in the mitochondrial membrane potential over 30 min (110±5% of the initial value, Fig. 5). However, the nonfluorescent mitochondrial uncoupler, compound 1799, decreased the mitochondrial membrane potential by 87±1% within 30 min, demonstrating that the membrane potential–sensitive dye, TMRE, was responding appropriately to changes in the mitochondrial membrane potential (Fig. 5). Using the substrates ADP and succinate to assess mitochondrial respiration, we obtained an acceptor control ratio (state 3 respiration/state 4 respiration) of 4.6, a value similar to that reported in the literature (32). In contrast to the lack of effect of GCDC on the mitochondrial membrane potential, GCDC inhibited state 3 mitochondrial respiration in a dose-dependent manner (Fig. 6). GCDC did not affect state 4 respiration (data not shown). TUDC had no effect on state 3 mitochondrial respiration (Fig. 6). Thus,

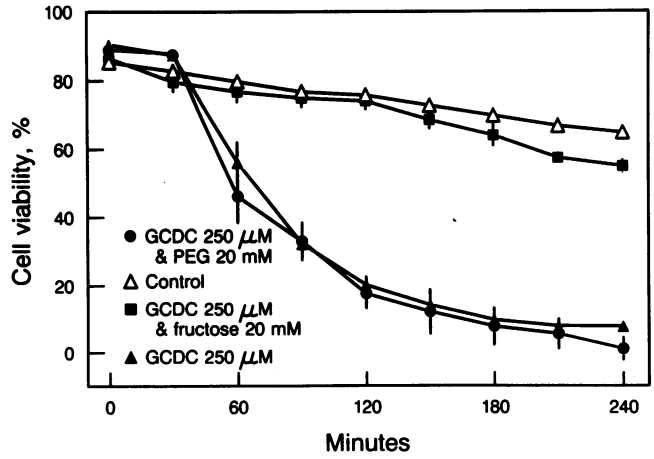

Figure 4. Fructose protects against cytotoxicity by GCDC. Hepatocyte suspensions (10^5/ml) were incubated in 3 ml of KRH buffer containing 1 μM propidium iodide and 0.2% BSA at 37°C. Cell viability was assessed by propidium iodide fluorometry. Cells were incubated in the presence (*closed triangles*) and absence (*open triangles*) of 250 μM GCDC, in the presence of 250 μM GCDC plus 20 mM fructose (*closed squares*), and in the presence of 250 μM GCDC plus 20 mM PEG (*closed circles*).

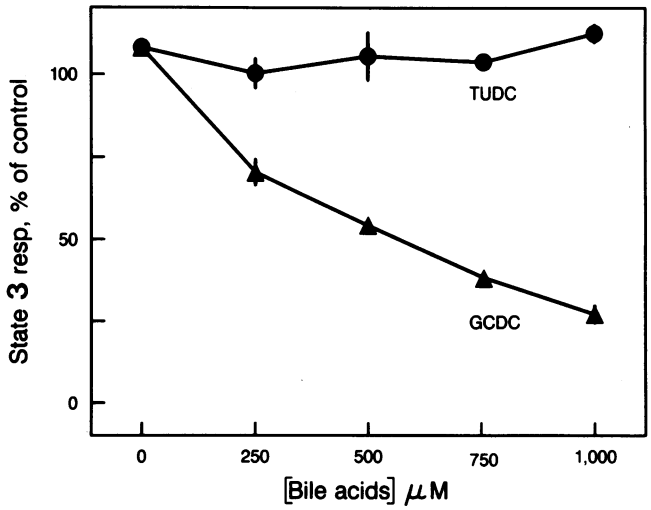

Figure 6. Concentration dependence of GCDC-mediated inhibition of state 3 mitochondrial respiration. Mitochondrial respiration was measured as oxygen consumption in hepatocyte suspensions permeabilized with 10 μM digitonin. Cells were suspended in buffer containing 1 mM ADP and 5 mM succinate, 5 μM rotenone, and various concentrations of GCDC (*closed triangles*), and TUDC (*closed circles*). Oxygen consumption was measured polarographically. Basal values for state 3 mitochondrial respiration were 181±8 ng-atm 0 min^1 10^6 cells.

GCDC specifically and directly impairs mitochondrial function by a mechanism that does not involve uncoupling of mitochondria.

GCDC increases Ca_i^{2+}. Ca_i^{2+} was measured in single, cultured hepatocytes loaded with fura-2 using multiparameter digitized video microscopy. The onset of cell death was identified by the abrupt loss of fura-2 fluorescence as previously reported (36). Basal values of Ca_i^{2+} were 222±30 nM, similar to the value of 247±53 nM reported by Tsien and co-workers (37). After treatment with 250 μM GCDC, Ca_i^{2+} remained stable before rising to 1,000–1,200 nM in a 60–180-min period preceding cell death (Fig. 7, *top*). To determine whether the source of Ca^{2+} responsible for the increase in Ca_i^{2+} was intra- or extracellular, experiments were performed using KRH buffer without added calcium. After treatment with 250 μM GCDC in the absence of added extracellular calcium, no rise in Ca_i^{2+} occurred over a 6-h period and loss of cell viability was not observed (Fig. 7). Finally, addition of 20 mM fructose to KRH buffer containing calcium also prevented the rise in cytosolic calcium and cell death after addition of 250 μM GCDC (Fig. 7, *bottom*). These results suggest that the increase in Ca_i^{2+} during GCDC cytotoxicity is dependent upon extracellular Ca^{2+} and a decrease in cellular ATP.

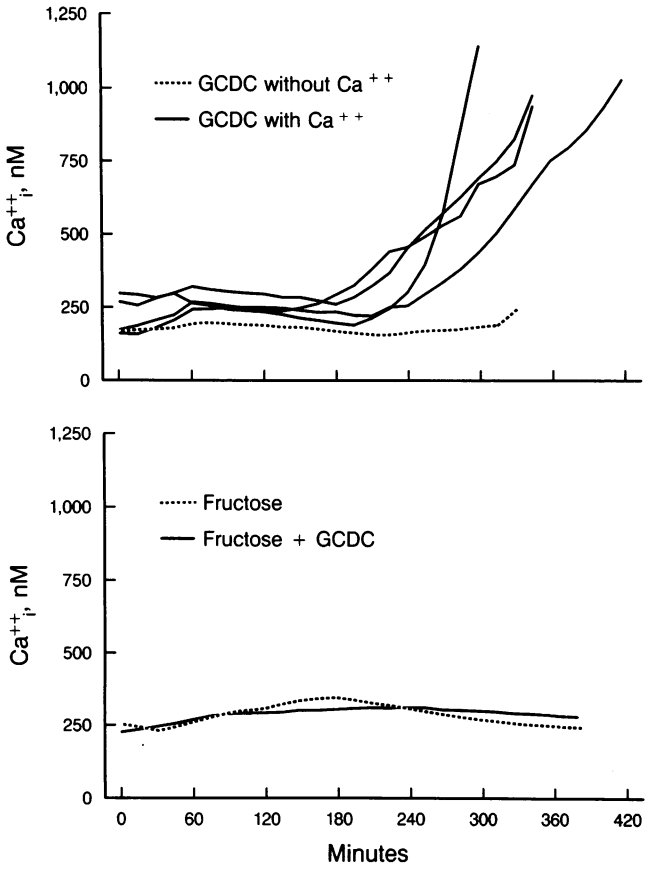

Figure 7. Ca_i^{2+} increases during exposure to GCDC and is dependent upon extracellular Ca^{2+} and ATP depletion. Ca_i^{2+} was monitored by ratio imaging of fura-2 fluorescence in isolated, cultured hepatocytes using multiparameter digitized video microscopy. (*Top*) GCDC-treated cells were incubated in KRH buffer in the presence (*solid lines*) and absence (*broken line*) of Ca^{2+} in the buffer. The four cells indicated by the solid lines are representative of numerous cells. The broken line represents the mean of eight separate cells from different experiments. (*Bottom*) Ca_i^{2+} was monitored in cells treated with fructose alone (*broken line*) and fructose plus GCDC (*solid line*) in KRH buffer containing Ca^{2+}. Each line represents the mean of data obtained from 15 cells.

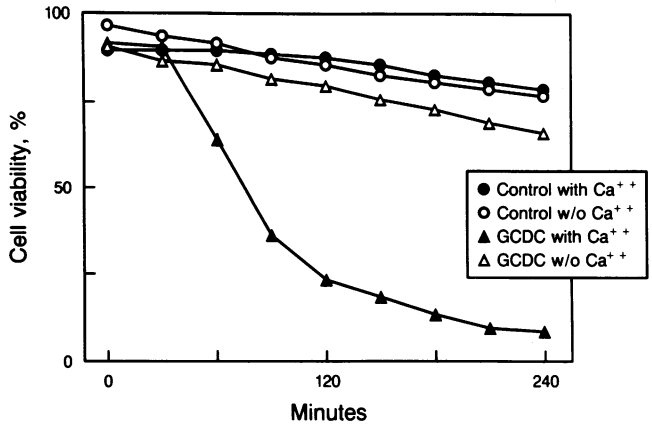

Figure 8. GCDC cytotoxicity is dependent upon extracellular calcium. Hepatocyte suspensions (10^5/ml) were incubated in 3 ml of KRH buffer containing 1 μM propidium iodide and 0.2% BSA at 37°C. Cell viability was assessed by propidium iodide fluorometry for cells in KRH buffer with (*closed circles*) and without (*open circles*) added extracellular calcium (2 mM), and cells treated with 250 μM GCDC in KRH buffer with (*closed triangles*) and without (*open triangles*) added extracellular calcium.

Removal of extracellular calcium protects against cell killing and inhibits cellular proteolysis during cytotoxicity by GCDC. Removal of Ca^{2+} from the suspension buffer prevented GCDC cytotoxicity (Fig. 8). After 2 h of exposure to 250 μM GCDC, cell viability was only 23±1% with extracellular Ca^{2+} compared with 80±1% in the absence of added extracellular Ca^{2+} ($P < 0.01$). The rise in Ca_i^{2+} during GCDC cytotoxicity is delayed until after 1 h (Fig. 7). Removal of extracellular calcium after 1 h of exposure to 250 μM GCDC and before the rise in Ca_i^{2+} also improved cell viability equal to that of cells treated with GCDC in Ca^{2+}-free media from the onset of the experiment (data not shown). Thus, GCDC-mediated cytotoxicity appears to be dependent upon an influx of extracellular Ca^{2+} into the cell leading to a rise in Ca_i^{2+}. Sustained increases in Ca_i^{2+} are thought to contribute to lethal cell injury by activating calcium-dependent proteases (18, 19, 24). Therefore, we measured cellular proteolysis in the presence and absence of extracellular calcium after addition of 250 μM GCDC. After 2 h, cumulative proteolysis was greater in the presence than in the absence of extracellular calcium, 1,299±11 vs. 876±7 nmol of TCA-soluble free amines/10^6 cells, respectively ($P < 0.01$, Fig. 9).

Extracellular acidosis protects against cell killing by GCDC. Lethal hepatocellular injury after ATP depletion is inhibited by extracellular acidosis by a mechanism dependent on intracellular acidification (38). In contrast, an acidic pH potentiates the membrane detergent effects of conjugated bile salts by protonating the carboxyl side chain, which renders the molecule more hydrophobic. For example, an acidic pH promotes hemolysis of red blood cells by bile salts (39). An acidic extracellular pH of 6.4 prevented cell killing by 250 μM GCDC (Fig. 10). After 4 h of incubation with GCDC, cell viability at pH 6.4 was 69±1% compared with a viability of 23±1% at pH 7.4 ($P < 0.01$) and was similar to controls at pH 7.4 or 6.4

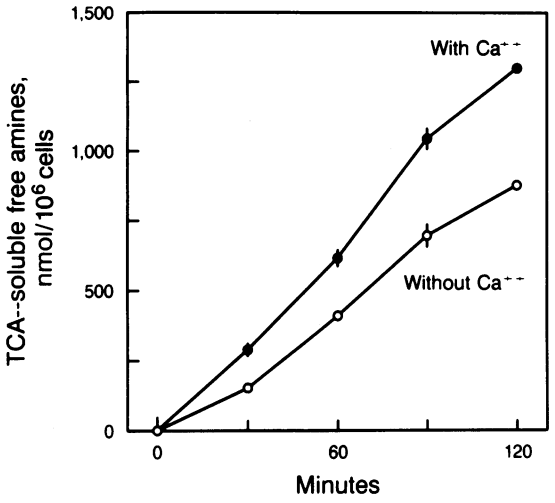

Figure 9. Cellular proteolysis during exposure to GCDC is dependent upon extracellular Ca^{2+}. Hepatocyte suspensions (10^5/ml) were incubated in 3 ml of KRH buffer at 37°C. Cells were treated with 250 μM GCDC in the presence (*closed circles*) and absence (*open circles*) of added extracellular calcium (2 mM). Total cellular proteolysis was quantitated as an increase in TCA-soluble free amines via a fluorescent assay using fluorescamine.

(71±1 and 74±1%). Likewise, an extracellular pH of 6.4 also protected hepatocytes against TCDC-mediated cytotoxicity. After 4 h of incubation with 250 μM TCDC, cell viability was 68±1% at pH 6.4 compared with 38±2% at pH 7.4, $P < 0.05$ (data not shown). Protection by an acidic pH suggests that ATP depletion rather than detergent-mediated membrane lysis is the primary mechanism of GCDC-mediated lethal hepatocellular injury at a concentration of 250 μM.

Discussion

The major findings of this study relate to the cellular mechanisms of lethal hepatocellular injury by GCDC, a primary bile salt. Our results demonstrate that lethal hepatocellular injury

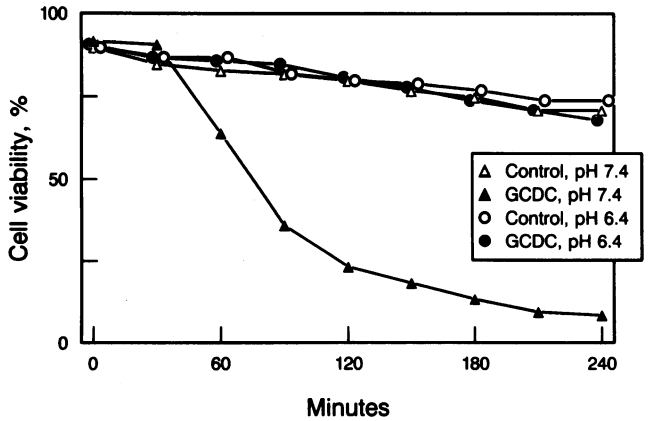

Figure 10. Extracellular acidosis protects against cytotoxicity by GCDC. Hepatocyte suspensions (10^5/ml) were incubated in 3 ml of KRH buffer containing 1 μM propidium iodide and 0.2% BSA at 37°C. Control and GCDC-treated (250 μM) cells were studied at pH 7.4 (*open* and *closed triangles*, respectively) and 6.4 (*open* and *closed circles*, respectively). Cell viability was assessed by propidium iodide fluorometry.

by GCDC is associated with a rapid and significant depletion of cellular ATP followed by a sustained increase in Ca_i^{2+}. In addition, GCDC cytotoxicity can be prevented by glycolytic production of ATP from fructose, removing extracellular calcium from the medium, and by an acidic extracellular pH. The results suggest that GCDC cytotoxicity results from hepatocellular ATP depletion leading to a subsequent rise in Ca_i^{2+}. The rise in Ca_i^{2+} may activate Ca^{2+}-dependent degradative enzymes which act as the final cytolytic trigger.

Serum bile salts in cholestasis are 0.1–0.3 mM in serum, but > 95% of GCDC and TCDC is bound to albumin and other proteins (9, 40); thus, unbound bile salt concentrations in serum are probably < 0.1 mM. In contrast, bile salt concentrations in the canaliculus are in the range of 5–50 mM. However, the most physiologically relevant concentration of bile salts to study in isolated cell preparations would be the intracellular concentration present in the hepatocyte during cholestasis. Hepatic tissue concentrations of bile salts have been measured in cholestasis. Although hepatic tissue consists predominantly of hepatocytes, it also contains bile canaliculi and bile ducts leading to an overestimate of the hepatocellular bile salt concentration. Nonetheless, these are the only data available. The hepatic tissue concentration of CDC in cholestasis is 415 nmol/g liver tissue (21). Assuming 100×10^6 hepatocytes/g wet weight and 5 μl of water/10^6 hepatocytes (41), the intracellular concentration of CDC and its conjugated species is ~ 800 μM based on measurements of hepatic tissue concentrations of CDC in cholestasis. Therefore, we were especially interested in the toxicity of bile salt concentrations below this value. Over the range of 0–500 μM, GCDC cytotoxicity was concentration dependent with near maximal killing at 250 μM. These results demonstrate that GCDC cytotoxicity in vitro occurs at bile salt concentrations probably relevant to those found within the hepatocyte in human disease.

Fructose, which provides ATP via glycolysis, protects against hepatocellular death by anoxia and mitochondrial toxins (27, 34, 35, 42, 43). Although glucose can also provide ATP by glycolysis, fructose is a more efficient glycolytic substrate than glucose in hepatocytes due to the high K_m of glucokinase for glucose and the low K_m of fructokinase for fructose (35, 44). In our studies, lethal hepatocellular injury by GCDC was associated with ATP depletion, and fructose protected against ATP depletion and cell killing. These findings strongly suggest that ATP depletion plays a pivotal role in GCDC-mediated lethal hepatocellular toxicity. Although fructose maintained ATP at concentrations of only 50% of the initial value, ATP concentrations of 20% of the initial value have been found to be protective during anoxic hepatocellular injury (34). Finally, glycolytic production of ATP by fructose demonstrates that glycolytic pathways are intact during GCDC cytotoxicity. Because ATP is only formed from glycolysis or mitochondrial oxidative phosphorylation, these data suggest that GCDC impairs mitochondrial function.

GCDC did not alter the mitochondrial membrane potential, demonstrating that mitochondria are not uncoupled during GCDC cytotoxicity. Although the mechanism of maintenance of the mitochondria membrane potential after ATP depletion is incompletely understood, previous studies have also observed preservation of the mitochondrial membrane potential during ATP depletion by anoxia and metabolic inhibition (45, 46). In contrast to the lack of effect of GCDC on the mitochondrial membrane potential, GCDC impaired state 3

mitochondrial respiration (substrate-stimulated respiration) but not state 4 respiration (substrate-independent respiration). The lack of effect of GCDC on state 4 respiration suggests that GCDC does not inhibit electron transport by the respiratory chain, but rather inhibits transport processes required for substrate-stimulated respiration. An inhibition of state 3 respiration has also been observed in mitochondria isolated from bile duct–ligated rats, an animal model of cholestasis associated with retention of bile salts (47). Thus, inhibition of mitochondrial function by GCDC and perhaps other bile salts appears to be a mechanism of liver injury during cholestasis.

GCDC cytotoxicity was associated with a sustained increase in Ca_i^{2+} in cultured hepatocytes. The rise in Ca_i^{2+} was abolished with removal of extracellular Ca^{2+}, indicating that an influx of calcium from the extracellular medium was responsible for the rise in Ca_i^{2+}. Our data demonstrating stimulation of calcium influx into the cell from the extracellular medium by GCDC, a dihydroxy bile salt, are consistent with previous observations. Although monohydroxylated bile salts release calcium from inositol triphosphate–sensitive intracellular pools causing an increase in Ca_i^{2+}, multihydroxylated bile salts do not (13). Moreover, Anwer and co-workers observed an increase in Ca_i^{2+} in hepatocytes dependent upon extracellular Ca^{2+} with a variety of dihydroxy bile salts (16). In our studies, we also found that fructose prevented the rise in Ca_i^{2+}, suggesting that the rise in Ca_i^{2+} could be prevented by maintaining cellular ATP concentration. Although the role of ATP depletion in causing a rise in Ca_i^{2+} during cell injury is controversial (45, 48), recent data suggest that ATP depletion is associated with increases of Ca_i^{2+} (35, 49). Moreover, bile salts have the additional effect of promoting calcium movement across biomembranes, liposomes, and synthetic membranes (14, 15, 17). The combination of ATP depletion and this calcium ionophore-like activity of bile salts may both be necessary for the rise in Ca_i^{2+} during GCDC cytotoxicity. The observation by others that the nontoxic bile salt, ursodeoxycholate, increases Ca_i^{2+}, but does not cause ATP depletion as shown in our studies, further supports the concept that both ATP depletion and increases in Ca_i^{2+} are required for cytotoxicity (50).

Loss of cell viability was measured in cell suspensions while Ca_i^{2+} was measured in individual, cultured hepatocytes. Ca_i^{2+} cannot be measured in hepatocyte suspensions using fura-2, because hepatocytes efficiently transport fura-2 into the extracellular medium and fluorescent measurements reflect principally extracellular Ca^{2+}. However, fura-2 can be used to measure Ca_i^{2+} in cultured hepatocytes using digitized video microscopy as only the intracellular fluorescence is quantitated (51). After exposure to GCDC, the time to cell death was prolonged in cultured cells as compared with cell suspensions. Prolonged survival in the cultured cells may be due to less efficient transport of bile salts by cultured hepatocytes (26). Despite the differences in time to death, the sequence of intracellular events appeared to be the same as calcium was important for cell death in both models. Indeed, removal of extracellular calcium prevented the rise in Ca_i^{2+} during GCDC cytotoxicity in cultured cells and prolonged cell survival in both cultured cells and cell suspensions.

Calcium-dependent, autolytic degradative proteolysis has been implicated in lethal hepatocellular injury (52, 53). Removal of extracellular Ca^{2+} inhibited proteolysis and protected against cell killing by GCDC. Our data suggest that calcium-mediated degradative proteolysis may play a key role in lethal hepatocellular injury by GCDC. Proteolysis may be lysosomal or nonlysosomal. Because lysosomal proteolysis can be expected to be suppressed during ATP depletion and cell injury (54, 55), it is reasonable to assume that calcium-dependent, nonlysosomal proteolysis contributes to lethal cell injury by GCDC. Indeed, an increase in calcium-dependent nonlysosomal proteolysis has been described as a mechanism for lethal hepatocellular injury by cystamine (53).

Our working hypothesis is that GCDC cytotoxicity is dependent on ATP depletion and a direct physicochemical interaction of the bile salt with the plasma membrane increasing calcium permeability. Initially, GCDC is transported into the hepatocyte where it impairs mitochondrial oxidative phosphorylation causing ATP depletion. In addition, GCDC appears to increase the plasma membrane permeability to extracellular Ca^{2+}, causing calcium to enter the cell. The increased membrane permeability to calcium may be due to a direct physicochemical effect of GCDC on the plasma membrane. Although the critical micellar concentration of bile salts is in the 2–3-mM range in electrolyte solutions, critical concentrations of bile salts for formation of mixed micelles with membrane lipids are much lower, 0.1–0.2 mM, and are associated with an enhanced permeability of membranes (56, 57). In the absence of ATP, failure of the plasmalemma and endoplasmic reticulum ATP-dependent calcium pumps would lead to a sustained rise in Ca_i^{2+}, activating degradative hydrolases such as nonlysosomal proteases, phospholipases, and endonucleases (58). Increased activity of these hydrolases leads to degradation of cellular proteins, membranes, DNA, and RNA, producing cell dysfunction and cell death. Our data, demonstrating that lethal hepatocellular injury by GCDC can be inhibited by preventing the rise in Ca_i^{2+} with fructose or removing extracellular Ca^{2+}, support this hypothesis. Although our initial studies identified calcium-dependent proteolysis during GCDC cytotoxicity, identifying the precise role of these proteases and of phospholipases and endonucleases in mediating GCDC cytotoxicity will require further work. The dependence on ATP depletion suggests that GCDC causes a bioenergetic form of lethal cell injury analogous to anoxic hepatocellular injury. Finally, this model provides a framework to determine the injurious effects of bile acids in cholestasis and the site(s) of cytoprotection by ursodeoxycholate.

Acknowledgments

The secretarial assistance of Marjorie Severeid is gratefully acknowledged. We thank Dr. R. K. Pearson for reviewing the manuscript and providing helpful comments.

This work was supported by grant DK-45331 from the National Institutes of Health, by Ciba-Geigy, and by the Mayo Foundation.

References

1. Scholmerich, J., M. S. Becher, K. Schmidt, R. Schubert, B. Kremer, S. Feldhaus, and W. Gerok. 1984. Influence of hydroxylation and conjugation of bile acids on their membrane-damaging properties: studies on isolated hepatocytes and membrane vesicles. *Hepatology.* 4:661–666.

2. Galle, P. R.; L. Theilmann, R. Raedsch, G. Otto, and A. Stiehl. 1990. Ursodeoxycholate reduces hepatotoxicity of bile salts in primary human hepatocytes. *Hepatology.* 12:486–491.

3. Schumucker, D. L., M. Ohta, S. Kanai, Y. Sato, and K. Kitani. 1990. Hepatic injury induced by bile salts: correlation between biochemical and morphological events. *Hepatology.* 12:1216–1221.

4. Quest, R. G., T.-T. Ton-nu, J. Lillienau, A. F. Hofman, and K. E. Barrett. 1991. Activation of mast cells by bile acids. *Gastroenterology.* 101:446–456.

5. Mekhjian, H. S., and S. F. Phillips. 1970. Perfusion of the canine colon with unconjugated bile acids: effect on water and electrolyte transport, morphology and bile acid absorption. *Gastroenterology.* 59:120–131.

6. Poupon, R. E., B. Balkan, E. Eschwege, and R. Poupon. 1991. A multicenter, controlled trial of ursodiol for the treatment of primary biliary cirrhosis. *N. Engl. J. Med.* 324:1548–1554.

7. Scharschmidt, B. F., E. B. Keeffe, D. A. Vessey, N. M. Blankenship, and R. K. Ockner. 1981. *In vitro* effect of bile salts on rat liver plasma membrane, lipid fluidity, and ATPase activity. *Hepatology.* 1:137–145.

8. Bilington, D., C. E. Evans, P. P. Godfrey, and R. Coleman. 1980. Effects of bile salts on the plasma membranes of isolated rat hepatocytes. *Biochem. J.* 88:321–323.

9. Raedsch, R., G. H. Lauterburg, and A. F. Hofmann. 1981. Altered bile acid metabolism in primary biliary cirrhosis. *Dig. Dis. Sci.* 26:395–400.

10. Crosignani, A., M. Podda, P. M. Battezzati, E. Bertolini, M. Zuin, D. Watson, and K. D. R. Setchell. 1991. Changes in bile acid composition in patients with primary biliary cirrhosis induced by ursodeoxycholic acid administration. *Hepatology.* 14:1000–1007.

11. Beuers, U., U. Spengler, F. M. Zwiebel, J. Pauletzki, S. Fischer, and G. Paumgartner. 1992. Effect of ursodeoxycholic acid on the kinetics of the major hydrophobic bile acids in health and in chronic cholestatic liver disease. *Hepatology.* 15:603–608.

12. Oelberg, D. G., W. P. Dubinsky, J. W. Sackman, L. B. Wang, E. W. Adcock, and R. Lester. 1987. Bile salts induce calcium uptake *in vitro* by human erythrocytes. *Hepatology.* 7:245–252.

13. Combettes, L., M. Dumont, B. Berthron, S. Erlinger, and M. Claret. 1988. Release of calcium from the endoplasmic reticulum by bile acids in rat liver cells. *J. Biol. Chem.* 263:2299–2303.

14. Abramson, I. I., and A. E. Shamoo. 1979. Anionic detergents as divalent cation ionophores across black lipid membranes. *J. Membr. Biol.* 50:241–244.

15. Maenz, D. D., and G. W. Forsyth. 1984. Calcium ionophore activity of intestinal secretory compounds. *Digestion.* 30:138–150.

16. Anwer, M. S., L. R. Engelking, K. Nolan, D. Sullivan, P. Zimniak, and R. Lester. 1988. Hepatotoxic bile acids increase cytosolic Ca^{++} activity of isolated rat hepatocytes. *Hepatology.* 8:887–891.

17. Zimniak, P., J. M. Little, A. Radominska, D. G. Oelberg, M. S. Anwer, and R. Lester. 1991. Taurine-conjugated bile acids act as Ca^{++} ionophores. *Biochemistry.* 30:8598–8604.

18. Jewell, S. A., G. Bellomo, H. Thor, S. Orrenius, and M. T. Smith. 1982. Bleb formation in hepatocytes during drug metabolism is caused by disturbances in thiol and calcium ion homeostasis. *Science (Wash. DC).* 217:1257–1259.

19. Trump, B. F., and F. Berezesky. 1985. The role of calcium in cell injury and repair: a hypothesis. *Surv. Synth. Pathol. Res.* 4:248–256.

20. Miyazaki, K., F. Nakayama, and A. Koga. 1984. Effect of chenodeoxycholic and ursodeoxycholic acids on isolated adult human hepatocytes. *Dig. Dis. Sci.* 12:1123–1130.

21. Greim, H., P. Czygan, F. Schaffner, and H. Popper. 1973. Determination of bile acids in needle biopsies of human liver. *Biochem. Med.* 8:280–286.

22. Kimura, T. 1980. Cytotoxicity of bile acids on cultured cells. *Nippon Shokakibyo Gakkai Zasshi.* 77:185–194.

23. Crosignani, A., M. Podda, P. M. Battezzati, E. Bertolini, M. Zuin, D. Watson, and K. D. R. Setchell. 1991. Changes in bile acid composition in patients with primary biliary cirrhosis induced by ursodeoxycholic acid administration. *Hepatology.* 14:1000–1007.

24. Groskreutz, J. L., S. F. Bronk, and G. L. Gores. 1992. Ruthenium red delays the onset of cell death during oxidative stress of rat hepatocytes. *Gastroenterology.* 102:1030–1038.

25. Bronk, S. F., and G. J. Gores. 1991. Acidosis protects against lethal oxidative injury of liver sinusoidal endothelial cells. *Hepatology.* 14:150–157.

26. Frimmer, M., and K. Ziegler. 1988. The transport of bile acids in liver cells. *Biochim. Biophys. Acta.* 947:75–99.

27. Gores, G. J., A.-L. Nieminen, K. E. Fleishman, T. L. Dawson, B. Herman, and J. J. Lemasters. 1988. Extracellular acidosis protects against the onset of cell death of ATP-depleted hepatocytes. *Am. J. Physiol.* 255:C315–C322.

28. Baker, P. R., J. C. Wilton, C. E. Jones, D. J. Stenzel, N. Watson, and G. J. Smith. 1992. Bile acids influence the growth, oestrogen receptor and oestrogen-regulated proteins of MCF-7 human breast cancer cells. *Br. J. Cancer.* 65:566–572.

29. Mashige, F., K. Imai, and T. Osuga. 1976. A simple and sensitive assay of total serum bile acids. *Clin. Chim. Acta.* 70:79–86.

30. Grynkiewicz, G., M. Poenie, and R. Y. Tsien. 1985. A new generation of Ca^{++} indicators with greatly improved fluorescence properties. *J. Biol. Chem.* 260:3440–3450.

31. Loew, L. M., D. L. Farkas, and M. Wei. 1990. Membrane potential imaging: ratios, templates and quantitative confocal microscopy. *In* Optical Microscopy for Biology. H. Herman and K. Jacobson, editors. Wiley-Liss, Inc., New York. 131–142.

32. Moreadith, R. W., and G. Fiskum. 1984. Isolation of mitochondria from ascites tumor cells permeabilized with digitonin. *Anal. Biochem.* 137:360–367.

33. Pacifici, R. E., and K. J. A. Davies. 1990. Protein degradation as an index of oxidative stress. *Methods Enzymol.* 186:485–502.

34. Anundi, I., and H. deGroot. 1989. Hypoxic liver cell death: critical pO2 and dependence of viability on glycolysis. *Am. J. Physiol.* 257:G58–G64.

35. Gasbarrini, A., A. B. Borle, H. Farghali, A. Francavilla, and D. Van Thiel. 1992. Fructose protects rat hepatocytes from anoxic injury. *J. Biol. Chem.* 11:7545–7552.

36. Nieminen, A.-L., G. J. Gores, T. L. Dawson, B. Herman, and J. J. Lemasters. 1990. Toxic injury from mercuric chloride in rat hepatocytes. *J. Biol. Chem.* 265:2399–2408.

37. Kawanishi, T., L. M. Blank, A. T. Harootunian, M. T. Smith, and R. Y. Tsien. 1989. Ca^{+2} oscillations induced by hormonal stimulation of individual fura-2-loaded hepatocytes. *J. Biol. Chem.* 264:12859–12866.

38. Gores, G. J., A.-L. Nieminen, B. E. Wray, B. Herman, and J. J. Lemasters. 1989. Intracellular pH during "chemical hypoxia" in cultured rat hepatocytes. Protection by intracellular acidosis against the onset of cell death. *J. Clin. Invest.* 83:386–396.

39. Ilani, A., and R. Granoth. 1990. The pH dependence of the hemolytic potency of bile salts. *Biochim. Biophys. Acta.* 1027:199–204.

40. Roda, A., G. Capelleri, R. Aldini, E. Roda, and L. Barbara. 1982. Quantitative aspects of the interaction of bile acids with human serum albumin. *J. Lipid Res.* 23:490–495.

41. Berry, M. N., A. M. Edwards, and G. J. Barritt. 1991. Biochemical properties. *In* Isolated Hepatocytes: Preparation, Properties, and Applications. R. H. Burdon, and P. H. van Knippenberg, editors. Elsevier Science Publishing Co., Inc., New York. 121–178.

42. Anundi, I., J. King, D. A. Owen, H. Schneider, J. J. Lemasters, and R. G. Thurman. 1987. Fructose prevents hypoxic cell death in liver. *Am. J. Physiol.* 253:G390–G396.

43. Nieminin, A.-L., T. L. Dawson, G. J. Gores, T. Dawanishi, B. Herman, and J. J. Lemasters. 1990. Protection by acidotic pH and fructose against lethal injury to rat hepatocytes from mitochondrial inhibitors, ionophores and oxidant chemicals. *Biochem. Biophys. Res. Commun.* 167:600–606.

44. Sols, A., M. Salas, and E. Vinuela. 1964. Induced biosynthesis of liver glucokinase. *Adv. Enzyme Regul.* 2:177–188.

45. Lemasters, J. J., J. DiGuiseppi, A.-L. Nieminen, and B. Herman. 1987. Blebbing, free Ca^{++} and mitochondrial membrane potential preceding cell death in hepatocytes. *Nature (Lond.).* 325:78–81.

46. Au, T. Y., B. S. Andersson, and D. P. Jones. 1987. Mitochondrial transmembrane ion distribution during anoxia. *Am. J. Physiol.* 252:2356–2361.

47. Krahenbuhl, S., J. Stucki, and J. Reichen. 1992. Reduced activity of the electron transport chain in liver mitochondria isolated from rats with secondary biliary cirrhosis. *Hepatology.* 15:1160–1166.

48. Orrenius, S., D. J. McConkey, and P. Nicotera. 1990. Role of calcium in toxic and programmed cell death. *In* Biological Reactive Intermediates IV. C. M. Witmer, R. R. Snyder, D. J. Jollow, G. F. Kalf, J. J. Kocsis, and F. I. Sipes, editors. Plenum Publishing Corp., New York. 419–425.

49. Nicotero, P., H. Thor, and S. Orrenius. 1989. Cytosolic free Ca^{++} and cell killing in hepatoma 1c1c7 cells exposed to chemical anoxia. *FASEB (Fed. Am. Soc. Exp. Biol.) J.* 3:59–64.

50. Beuers, U., M. H. Nathanson, and J. L. Boyer. 1992. Tauroursodeoxycholic acid (TUDCA) modulates signal transduction pathways that influence intracellular Ca^{++}. *Gastroenterology.* 102:782a. (Abstr.)

51. Cobbold, P. H., and T. J. Rink. 1987. Fluorescence and bioluminescence measurement of cytoplasmic free calcium. *Biochem. J.* 248:313–328.

52. Lee, K. S., S. Frank, P. Vanderklish, A. Arai, and G. Lynch. 1991. Inhibition of proteolysis protects hippocampal neurons from ischemia. *Proc. Natl. Acad. Sci. USA.* 88:7233–7237.

53. Nicotera, P., P. Hartzell, C. Baldi, S. A. Svensson, G. Bellomo, and S. Orrenius. 1988. Cystamine induces toxicity in hepatocytes through elevation of cytosolic Ca^{++} and the stimulation of a nonlysosomal proteolytic system. *J. Biol. Chem.* 261:14628–14636.

54. Yamazaki, K., and N. F. LaRusso. 1989. The liver and intracellular digestion: how liver cells eat. *Hepatology.* 10:877–886.

55. Yu, Q. C., and L. Marzella. 1988. Response of autophagic protein degradation to physiologic and pathologic stimuli in rat hepatocyte monolayer cultures. *Lab. Invest.* 58:643–652.

56. Small, D. M. 1971. The physical chemistry of cholanic acids. *In* The Bile Acids: Chemistry, Physiology, and Metabolism. Vol. I. P. P. Nair and D. Kritchevsky, editors. Plenum Publishing Corp., New York. 249–356.

57. Schubert R., and K.-H. Schmidt. 1988. Structural changes in vesicle membranes and mixed micelles of various lipid compositions after binding of different bile salts. *Biochemistry.* 27:8787–8794.

58. Trump, B. F., and I. K. Berezesky. 1992. The role of cytosolic Ca^{++} in cell injury, necrosis and apoptosis. *Curr. Opin. Cell Biol.* 4:227–232.